J|A|C|S
ARTICLES
Published on Web 12/27/2005

Sliding Behavior of Water Droplets on Flat Polymer Surface

Naoya Yoshida,* Yuu Abe, Hiroaki Shigeta, Akira Nakajima,† Hisashi Ohsaki, Kazuhito Hashimoto, and Toshiya Watanabe

Contribution from the Research Center for Advanced Science and Technology, The University of Tokyo, 4-6-1 Komaba, Meguro-ku, Tokyo 153-8904, Japan, and Tokyo Institute of Technology, 2-12-1 O-okayama, Meguro-ku, Tokyo 152-8552, Japan

Received January 30, 2005; E-mail: naoya@wlab.rcsat.u-tokyo.ac.jp

Abstract: Flat films of methyl methacrylate−fluoroalkyl methacrylate copolymers were prepared, and their hydrophobicity was investigated. It was revealed that the F concentration directly affects the static hydrophobicity on the flat polymer surface in a systematic manner. Furthermore, the sliding behavior of a water droplet on these surfaces depends on the static hydrophobicity; the sliding motion changes from constant velocity to constant acceleration with an increase in the water contact angle.

Introduction

Static hydrophobicity can be controlled by surface energy and roughness. However, it is difficult to simultaneously control both static and dynamic hydrophobicities. To the best of our knowledge, while the sliding angle has been extensively reported,[1−5] there are only a few reports on sliding behavior.[6−9] It is expected that the sliding properties improve with an increase in the static hydrophobicity (decrease in the contact area and frictional resistance); however, it is well-known that they have no direct correlation.[10−12] This is probably because in practice, the difficulty in preparing samples with both well-defined surface energy and roughness as well as the lack of information on these controlling factors hamper the interpretation of the sliding phenomena. We consider that a small roughness of a few nanometers, which is insignificant in terms of static hydrophobicity, may significantly affect the dynamic hydrophobicity. The importance of roughness has been discussed from the viewpoint of the relation between the sliding angle and contact angle hysteresis[2−5] and that between roughness and hysteresis.[3,13] In fact, Morimoto et al. showed the dependence of the sliding angle on surface roughness.[14] Gupta et al. reported the water contact angle (WCA) hysteresis on self-assembled monolayers of alkanethioles on ultrasmooth gold; these monolayers showed an extremely small hysteresis.[15] Regarding the sliding velocity on superhydrophobic surfaces, Nakajima et al.[8] reported that a sliding water droplet had an extremely high constant acceleration, and Richard and Quere[9] reported the constant velocity of a sliding glycerol droplet. With regard to hydrophobic surfaces, only Nakajima et al.[6,7] provided in-depth reports on the sliding behavior of a droplet with varying size on flat 1*H*,1*H*,2*H*,2*H*-perfluorodecyltrimethoxysilane (FAS)-coated and octadecyltrimethoxysilane (ODS)-coated Si wafers. Although static hydrophobicity can be easily controlled by controlling the chemical composition and surface texture, the control of sliding behavior is still difficult. In the present study, we prepared flat films of methyl methacrylate (MMA)−fluoroalkyl methacrylate (FMA) copolymers and examined the relationship between static hydrophobicity and sliding behavior.

Experimental Section

The general procedures for preparing copolymers and their films are as follows: A solution of the methacrylate monomers (total of 10 mmol) and azobis(2,4-dimethylvaleronitrile) (0.50 mmol) in 2-butanone (1.1 mL) was stirred and heated in an oil bath at 60−70 °C for 1−6 h under N_2. The molecular weights of the copolymers were monitored by GPC−HPLC (TOSOH HLC-8120GPC system using a differential refractive index detector with TSKgel GMH_{HR}-L and GMH_{HR}-H columns with acetone as an eluent); the molecular weight of the obtained copolymers was approximately $M_W = 5 \times 10^4$. The products were characterized by ^{1}H NMR spectra recorded in a $CDCl_3$ solution by a JEOL AL400 spectrometer. The coating film was prepared on a soda-lime glass substrate (5 × 7 cm) by spin-coating (1500 rpm and 10 s); the film was prepared from a 2-butanone or 1,3-bis(trifluoromethyl)benzene (for FMA homopolymers) solution (20 g/L), and the obtained film was dried at 120 °C for 1 h.

X-ray photoelectron spectroscopy (XPS) measurements were conducted by a Physical Electronics (PHI) model 5600 spectrometer

† Tokyo Institute of Technology.

(1) Quere, D.; Azzopardi, M.-J.; Delattre, L. *Langmuir* **1998**, *14*, 2213−2216.
(2) Furmidge, C. G. L. *J. Colloid Sci.* **1962**, *17*, 309−324.
(3) Johnson, R. E., Jr., Dettre, R. H. *Surface and Colloid Science*; Matijevic, E., Ed.; Wiley: New York, 1969; Vol. 2, pp 85−153.
(4) Carre, A.; Shanahan, M. E. R. *J. Adhes.* **1995**, *49*, 177−185.
(5) Wolfram, E.; Faust, R. In *Wetting, Spreading and Adhesion*; Paddy, J. F., Ed.; Academic Press: New York, 1978, pp 213−222.
(6) Suzuki, S.; Nakajima, A.; Kameshima, Y.; Okada, K. *Surf. Sci.* **2004**, *557*, L163−L168.
(7) Nakajima, A.; Suzuki, S.; Kameshima, Y.; Yoshida, N.; Watanabe, T.; Okada, K. *Chem. Lett.* **2003**, 1148−1149.
(8) Miwa, M.; Nakajima, A.; Fujishima, A.; Hashimoto, K.; Watanabe, T. *Langmuir* **2000**, *16*, 5754−5760.
(9) Richard, D.; Quere, D. *Europhys. Lett.* **1999**, *48*, 286−291.
(10) Kamitani, K.; Teranishi, T. *J. Sol.-Gel Sci. Technol.* **2003**, *26*, 823−823.
(11) Murase, H.; Fujibayashi, T. *Prog. Org. Coat.* **1997**, *31*, 97−104.
(12) Murase, H.; Nanishi, K.; Kogure, H.; Fujibayashi, T.; Tamura, K.; Haruta, N. *J. Appl. Polym. Sci.* **1994**, *54*, 2051−2062.
(13) Youngblood, J. P.; McCarthy, T. J. *Macromolecules* **1999**, *32*, 6800−6806.
(14) Morimoto, T.; Sanada, Y.; Tomonaga, H. *Thin Solid Films* **2001**, *392*, 214−222.
(15) Gupta, P.; Ulman, A.; Fanfan, S.; Korniakov, A.; Loos, K. *J. Am. Chem. Soc.* **2004**, *127*, 4−5.

10.1021/ja050617m CCC: $33.50 © 2006 American Chemical Society

equipped with a hemispherical capacitor analyzer. The C, F, and Si atomic percentages were determined after including the appropriate instrumental sensitivity factors. Atomic force microscope (AFM) measurements were performed using an SPA300 (Seiko Instruments Inc.) in the noncontact mode. Microfabricated silicon cantilevers with a bending spring constant of 20 N/m (SI-DF3-A, Seiko Instruments) were used for imaging in air with a 20-μm scanner with a scan rate of 1.0 Hz.

The static contact angles were measured by a contact angle meter CA-X (sessile drop method, Kyowa Interface Science Co. Ltd., Japan). The surface energy containing polar and nonpolar terms was evaluated on the basis of the measured contact angles of water and CH_2I_2 (3 μL).[16] All the static contact angles were obtained as an average of five measurements.

The sliding angle was measured by a contact angle meter CA-X and a sliding system SA-11 (Kyowa Interface Science Co. Ltd.) with a water droplet of 30 μL. The water droplet was placed on a horizontal coating plate; the plate was then gradually inclined until the droplet (both the advancing and receding contact lines) began to slide, and the tilted angle was considered as the sliding angle.

The dynamic contact angle hysteresis and sliding motion were measured as follows: The 30-μL droplet was gently dropped on the surface inclined at 35°, and the sliding motion was then recorded every 1/30 s by a digital video camera (DCR-TRV50, Sony, Japan). The length of the samples (corresponding to the field of vision of the camera) was approximately 4 cm. The images at the beginning of sliding were analyzed by the FAMAS software (ver. 1.8.0, Kyowa Interface Science), thereby determining the advancing (θ_{ad}) and receding (θ_{rec}) contact angles of the sliding water droplet on the surface inclined at 35°. The sliding motion was analyzed by measuring the sliding distance of the front edge of the contact line between the droplet and the sample surface. The acceleration constant was calculated from a constant acceleration region by least-squares fitting using a quadratic equation.

Results and Discussion

We prepared MMA−FMA random copolymers ($M_W = \sim 5 \times 10^4$) by changing both the ratio (0−100%) and the fluoroalkyl chain length of FMA by radical polymerization in a systematic manner (Supporting Information: Table S1). The FMAs used were 2,2,2-trifluoroethyl methacrylate (FMA-F3), 2-(perfluorobutyl)ethyl methacrylate (FMA-F9), 2-(perfluorohexyl)ethyl methacrylate (FMA-F13), 2-(perfluorooctyl)ethyl methacrylate (FMA-F17), and 2-(perfluoro-7-methyloctyl)ethyl methacrylate (FMA-F19). The 2-butanone solutions of copolymers (1,3-bis(trifluoromethyl)benzene solutions for FMA homopolymers) were coated on the glasses by spin-coating (1500 rpm and 10 s) and then dried at 120 °C for 1 h; thus, colorless transparent films with a thickness of approximately 0.1 μm were obtained. The smoothness of the surface (Ra = 0.3−0.5 nm and Rz = 2.0−2.9 nm, Supporting Information: Figure S1) without any protuberances and with only small waving was verified by the AFM and laser microscopy; further, the heat-curing process may have caused a leveling effect due to the low melting points of the copolymers (below 120 °C). XPS 2D mapping[17] revealed the chemical homogeneity of the surface in the order of a few 10 μm; hence, high homogeneity may be derived from random copolymerization.

The surface analysis was carried out by XPS. The XPS spectra of the sample surfaces showed only C, F, and O peaks derived from the polymer, and Si from the glass substrate was not observed in any of the samples; therefore, the surface was completely covered with the polymer without any pinholes. The atomic concentrations of F and C were evaluated from these XPS spectra after including the appropriate instrumental sensitivity factors. Since the surface impurities were not removed experimentally and analytically, the intensity of the C signal may be enhanced to some extent; however, this systematic error may be small and may not significantly affect the results. The dependence of the WCA and surface energy on the F/(F + C) ratio (hereafter represented as surface coverage) is shown in Figure 1. This figure shows the simple relation of these parameters with the concentration of F at the surface, depending on the surface coverage and not on the fluoroalkyl chain length, with the exception of FMA-F3.

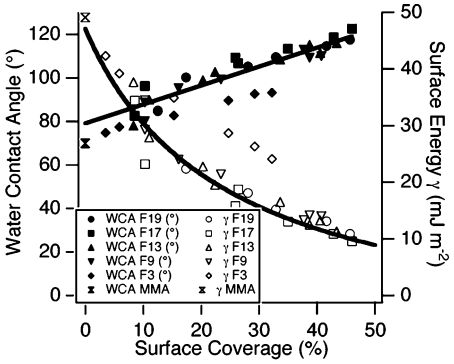

Figure 1. Relation between surface coverage F/(F + C) (%) and water contact angle (°) or surface energy (10^{-3} J/m^2).

The WCA showed a linear relation with surface coverage from 70° (PMMA) to approximately 120° (polyFMA-F19 and polyFMA-F17). The surface energy simply decreased from 50 to 10 mJ/m^2 with an increase in the surface coverage. The reported values of maximum WCA and minimum surface energy correspond to the obtained values of 120° and 10 mJ/m^2, respectively.[18] The theoretical maximum value of surface coverage is 66.7% for perfluoroalkane (C_nF_{2n+2}). In practice, the experimental maximum should be smaller than the theoretical one because the detection depth by XPS analysis includes not only fluoroalkyl chains but also polymethacrylate main chains. In this regard, the surfaces of most hydrophobic samples are believed to be almost completely covered with fluorine atoms from the fluoroalkyl chain. FMA-F3 has an extremely short chain length such that the F atoms cannot effectively cover the surface. This is probably because a shorter chain would be easily buried in the polymer main chain, which prevents the influence of surface energy. Therefore, the effect of the surface coverage of FMA-F3 appears to be weaker than that of other FMAs. This simple dependence of static WCA on surface coverage suggests that the effect of molecular structure and length, which strongly decrease the surface energy irrespective of F concentration at the surface, is not significant; this is observed in structures such as those with a very close packing (crystallization) of longer chains.

The sliding behaviors of the water droplet on these surfaces were evaluated. The droplet (30 μL) was gently dropped on the surface inclined at 35°; the sliding motion (distance: ~3 cm and time: ~0.1−5 s) was then recorded and analyzed.

(16) Owens, D. K. *J. Appl. Polym. Sci*. **1969**, *13*, 1741−1747.
(17) XPS 2D mapping was carried out by a model 5600 spectrometer (Physical Electronics) and ESCALAB220i-XL (Vacuum Generator) with lateral resolution of 10 μm.
(18) Nishino, T.; Meguro, M.; Nakamae, K.; Matsushita, M.; Ueda, Y. *Langmuir* **1999**, *15*, 4321−4323.

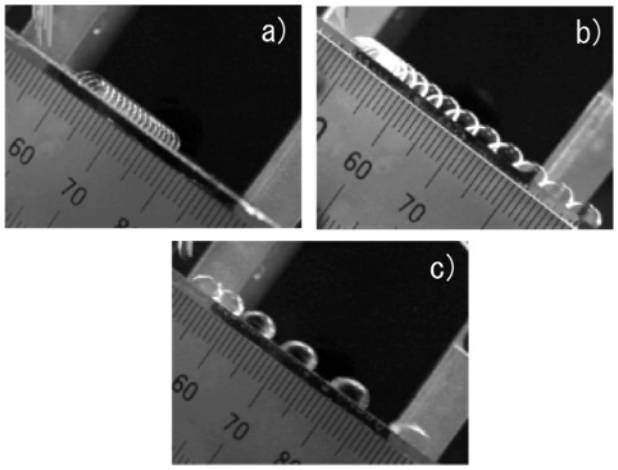

Figure 2. Typical sliding motions at constant velocity (FMA-F19 1%−MMA 99%) (a), constant velocity to constant acceleration (FMA-F13 6%−MMA 94%) (b), and constant acceleration (FMA-F19 25%−MMA 75%) (c).

Figure 2 (and Supporting Information: Figure S2) shows the typical sliding motions. The sliding motion changed from constant velocity to constant acceleration depending on the WCA of the sample. In the region with a lower WCA, the sliding droplet exhibited a constant velocity (Figure 2a). On the contrary, in the region with a higher WCA, the sliding droplet moved quickly and exhibited constant acceleration, as shown in Figure 2c. In the medium region (WCA: 90−100°, surface energy: 20−30 mJ/m^2), the sliding motion changed from constant velocity to constant acceleration by an unknown trigger. In the typical case of a FMA-F13 6%−MMA 94% surface, it was observed that the contact angle hysteresis (advancing contact angle − receding contact angle, degrees) instantaneously decreased from 30° to 4° at the point of change in the sliding motion. It is unclear what triggers this decrease in the hysteresis; however, the resultant decrease in three phase line length (or contact area) may change the sliding behavior. In particular, this behavior was also observed in FMA-F13 75%−MMA 25% and FMA-F13 100%. Furthermore, the velocity observed in the constant velocity region showed an inconsistent value for every measurement even on the same sample. The constant velocity at the medium region may be more sensitive to the surface conditions; however, the sliding distance with regard to constant velocity was ∼0.5 cm in every case; this distance was almost equal to the diameter of the water droplet. This implies that the constant velocity was affected by the changes in the surface structure and surface energy due to the permeation of water into the polymer film. The sliding accelerations are summarized in Figure 3. In this figure, it is clear that sliding acceleration has a simple relation with the surface energy.

In contrast, both the sliding angle and dynamic contact angle hysteresis determined at a surface inclination of 35° (from the images at the beginning of sliding) appear to depend on the chemical structure of the polymer, not on the static WCA, while the sliding angle alone directly depended on the contact angle hysteresis as reported (Figure 4 and see Supporting Information: Figure S3).[2−5] Figure 4 exhibits a relation between the slopes [$\Delta(\cos\theta_{rec} - \cos\theta_{ad})/\Delta$WCA] and the number of F atoms: −0.034 ± 0.002 (FMA-F19), −0.022 ± 0.005 (FMA-F17), −0.003 ± 0.002 (FMA-F13), 0.008 ± 0.004 (FMA-F9), and −0.008 ± 0.002 (FMA-F3). In the longer and shorter

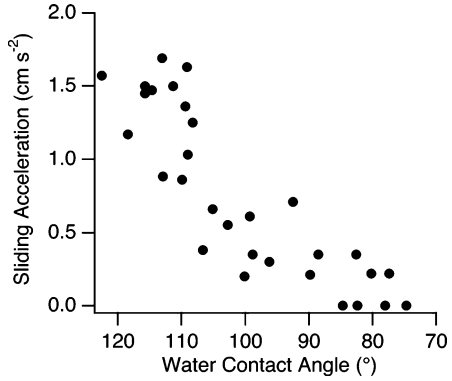

Figure 3. Plot of sliding acceleration (m/s^2) against water contact angle (°).

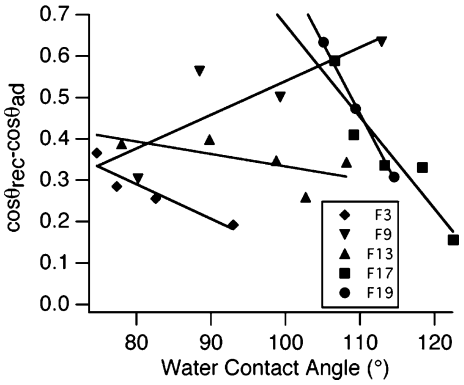

Figure 4. Contact angle hysteresis ($\cos\theta_{rec} - \cos\theta_{ad}$). ●: FMA-F19−MMA, ■: FMA-F17−MMA, ▲: FMA-F13−MMA, ▼: FMA-F9−MMA, and ◆: FMA-F3−MMA copolymers.

fluoroalkyl chains (FMA-F19, F17, and F3), it was evident that the dynamic contact angle hysteresis decreased with an increase in the FMA concentration (increase in WCA), while in the medium-length chain (FMA-F13 and F9), the decreasing or increasing effect was weak. This can be attributed to the aggregation effect of the longer fluoroalkyl chain (FMA-F19 and F17) and the larger reorientation of the medium chain (FMA-F13 and F9) at the water/polymer interface, as reported by Takahara et al.[19] The reorientation of the shortest chain (FMA-F3) may be very small because of its small orientation freedom. As shown here, the dynamic contact angle hysteresis did not affect the sliding acceleration. Therefore, it is suggested that the sliding angle (or the contact angle hysteresis) and sliding acceleration are mainly controlled by different factors.

Carre and Shanahan derived the following equation to describe the capillary force f against the direction of drop motion on an inclined hydrophobic plane.[4]

$$f \cong \frac{1}{2}\pi r\gamma_{LV}(\cos\theta_{rec} - \cos\theta_{ad}) = \frac{1}{2}\pi^{2/3}\gamma_{LV}\sin\theta\left[\frac{3V}{(2+\cos\theta)(1-\cos\theta)^2}\right]^{1/3} \times (\cos\theta_{rec} - \cos\theta_{ad}) \quad (1)$$

where r and V are the radius and volume of the water droplet, respectively, γ_{LV} is the surface tension of water, and θ is the

(19) Honda, K.; Morita, M.; Otsuka, H.; Takahara, A. *Macromolecules* **2005**, *38*, 5699−5705.

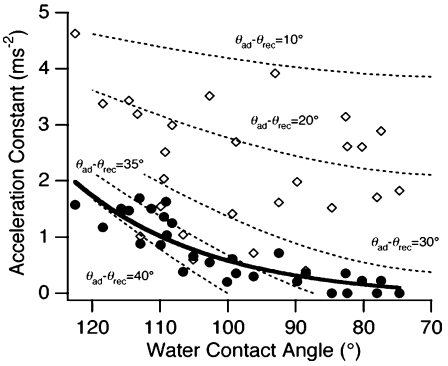

Figure 5. Calculated and experimental acceleration constants. Solid line is a fitting curve to the experimental data. Dotted lines are calculated acceleration constants from eq 2 at $\theta_{rec} - \theta_{ad}$ values of 10, 20, 30, 35, and 40°. ◇: Calculated acceleration constants from eq 2 with the hysteresis observed at 35°. ●: Experimental data.

contact angle on the horizontal plane. Assuming a very high Reynolds number, we neglected the viscous forces. The viscous force for a droplet of cylindrical shape was calculated as $6\eta^{\upsilon}/_{\theta}$ $\ln(x_{max}/x_{min})$, where η and υ are the viscosity of water and the velocity of a droplet, respectively, x_{max} is the macroscopic cutoff ($x_{max} \approx 2r \approx 0.5$ cm), and x_{min} is the molecular size.[20] This value is calculated as $\ll 1$; this value is too small against g sin 35° (= 5.6). In fact, the sliding behavior of constant acceleration indicated that the viscous forces depending on velocity are negligible, at least in these conditions.

Therefore, the external force F acting on the water droplet when sliding on the plate inclined at angle α may be approximated by the following equation:

$$F = ma = mg \sin \alpha - f \qquad (2)$$

where a is the sliding acceleration constant. Figure 5 shows the calculated (open diamonds and broken lines) and experimental (filled circles) acceleration constants. The broken lines are traced by plotting the constant hysteresis values ($\theta_{ad} - \theta_{rec}$) against the WCA, and the open diamonds represent the calculated acceleration constants by eq 2 (with the hysteresis value at $\alpha = 35°$) against WCA. In practice, eq 2 does not entirely fit the obtained experimental data, although the slopes (acceleration constant/WCA) are almost similar to the calculated lines with constant hysteresis values. The sliding motions with constant acceleration (see Supporting Information: Figure S2) suggested that the acceleration of the droplet was restricted by other resistance forces that are almost constant. Equation 2 gives a good fitting when the contact angle hysteresis is large ($\theta_{ad} - \theta_{rec} = 30-40°$); however, the calculated values are considerably larger when the hysteresis is smaller ($\theta_{ad} - \theta_{rec} < 30°$). Assuming the rolling of a droplet, we found that the rotational moment ($^2/_5 mr^2\omega$ for a rigid sphere, where ω is the angular velocity) was very low as well due to the residual resistance forces.

When the capillary force f was estimated with Wolfram's equation [$f = \pi r\gamma_{LV}/m(\cos\theta_{rec} - \cos\theta_{ad})$] for a circular drop,[5] f was calculated to be too large, and the calculated acceleration constant was negative in many cases. Furmidge's equation[2] for a parallel-sided drop ($f = \pi\omega\gamma_{LV}/m(\cos\theta_{rec} - \cos\theta_{ad})$, width of the droplet, ω, was calculated according to estimation by Dussan V and Chow[21]) yields a considerably larger "adhesion" force. The capillary force f is known to be extremely sensitive to the droplet shape, as suggested by many previous studies. This implies that the sliding motion cannot be only explained on the basis of the wide range of the WCA; however, as suggested by our observation, the sliding acceleration constant is strongly affected by the radius of the water droplet that is directly affected by the WCA. Although the cause of the residual forces is not entirely clear, they can be attributed to the interactions between the water and polymer molecules, complicated internal viscous motions, and so forth.

The surfaces in our samples clearly differ from the FAS-coated surface (conelike roughness).[22] The roughness of the FAS-coated surface is characteristic, although it is negligible with regard to the static contact angle because its roughness factor is sufficiently small. However, the resistance around the convexes may strongly affect the dynamic hydrophobicity due to the enhanced contact angle hysteresis. In fact, on the smooth surfaces of our samples without such convexes, the sliding behavior was satisfactory and could be explained by the relation with static hydrophobicity. The results also indicated that the smaller but sharp roughness, which is often observed on an FAS-coated surface, may severely affect the sliding property. Additionally, a change in sliding behavior, which is reported in ref 7, is observed to some extent. It is probable that the sliding behavior changed from slipping to rolling at a WCA of ~100° (surface energy: 20 mJ/m^2).

In summary, we prepared flat films of MMA−FMA copolymers with different fluoroalkyl chain lengths and FMA ratios and investigated their hydrophobicity. We demonstrated that the F-concentration directly affects the static hydrophobicity on a flat polymer surface in a systematic manner. Furthermore, the sliding behavior of a water droplet on these flat surfaces depends on the static hydrophobicity, where the sliding motion changes from constant velocity to constant acceleration with a decrease in the surface energy. Therefore, it is revealed that the sliding behavior can be simply controlled by the F-concentration on a highly smooth surface. It is noteworthy that the static and dynamic hydrophobicities (water contact angle, sliding angle, contact angle hysteresis, and sliding motion) can be controlled by modeling the chemical structure of the surface: The surface of a short fluoroalkyl chain copolymer exhibits small values of the WCA, contact angle hysteresis, sliding angles, and acceleration, while that of a medium fluoroalkyl chain copolymer exhibits medium values of the WCA and acceleration and large values of contact angle hysteresis and sliding angle. In a long fluoroalkyl chain copolymer (with a high FMA concentration), the surface exhibits large values of WCA and acceleration and small values of contact angle hysteresis and sliding angle.

Acknowledgment. The present research is supported by the "Advanced Technology Initiative for New Industry Creation" from the Ministry of Economy, Trade, and Industry of Japan. It is also supported in part by the Tokuyama Science Foundation and a grant for 21st Century COE Program "Human-Friendly Materials based on Chemistry" from the Ministry of Education,

(20) Brochard, F. *Langmuir* **1989**, *5*, 432−438.
(21) Dussan V, E. B.; Chow, R. T.-P. *J. Fluid Mech.* **1983**, *137*, 1−29.
(22) Pellerite, M. J.; Wood, E. J.; Jones, V. W. *J. Phys. Chem. B* **2002**, *106*, 4746−4754.

Culture, Sports, Science, and Technology of Japan. We thank Prof. T. Yokoyama, Dr. K. Takahashi, and Dr. T. Nakagawa (Institute of Molecular Science, Japan) for measuring the XPS mapping. We also thank Dr. M. Sakai for fruitful discussions on the sliding behavior.

Supporting Information Available: Details of surface properties. This material is available free of charge via the Internet at http://pubs.acs.org.

JA050617M